Hard-Sphere Interactions between Spherical Domains in Diblock Copolymers

David J. Kinning and Edwin L. Thomas*

Department of Polymer Science and Engineering, University of Massachusetts, Amherst, Massachusetts 01003. *Received September 13, 1983*

ABSTRACT: Small-angle scattering data from diblock copolymer systems containing disordered arrangements of spherical domains are modeled with the Percus–Yevick hard-sphere liquid theory to obtain the interparticle interference contribution to the scattered intensity. By choosing an effective hard-sphere interaction radius based on fitting the lowest angle interference peak and a domain radius from the location of the higher angle form factor scattering peaks, the full scattering pattern can be quite adequately accounted for. The difference between the hard-sphere radius and the domain size is attributed to the closest distance of approach between domains and corresponds to approximately 1.5 times the matrix block chain unperturbed radius of gyration. Thus, small-angle scattering data can provide a measurement of the separation distance at which the interdomain potential becomes highly repulsive.

Introduction

The introduction of anionic polymerization methods by Szwarc[1] in 1956 enabled well-defined block copolymers to be produced for the first time. Since then, a considerable amount of research has examined their properties, particularly those features connected with phase separation. Since the chemical species comprising the different blocks can be highly incompatible, (e.g., polystyrene–polydiene copolymers), the system will phase separate. However, due to the chemical linking of the blocks to each other, the scale of phase separation is restricted to occur with characteristic dimensions typically of several hundred angstroms, depending on the molecular weight of the blocks. Most morphological research has considered polystyrene–polydiene block copolymers, since these have been the most important commercially, but studies on other amorphous systems show the same general features.

Microphase separation usually results in the formation of domains of three geometries: spheres, cylinders, or lamellae, the geometry being determined in large part by the relative volume fractions of the components.[2] Morphological studies using both electron microscopy and small-angle scattering techniques have shown that under near-equilibrium conditions, the domains can be regularly arranged with lamellar domains of alternating layers of uniform spacing[3-7], cylindrical domains packed on a two-dimensional hexagonal lattice,[5,6,8] or spherical domains arranged on three-dimensional cubic lattices.[9,10]

Although an ordered arrangement of the domains is thought to be thermodynamically favored over a disordered arrangement,[11] disordered structures are often observed in systems with spherical domains, especially with the addition of homopolymer to the matrix.[12-21] An ordered lattice arrangement of domains will manifest itself as a series of distinct interference peaks at well-defined scattering angles. For nearly identical domains, sphere form factor scattering will give rise to several broad peaks at higher scattering angle. Small-angle data exhibiting several well-defined peaks both at low and high angle for spherical domain diblock copolymer systems is rare, especially for high molecular weight samples,[19-23] most probably due to nonequilibrium structures frozen in during the phase separation process during solvent casting, the usual method of sample preparation for small-angle scattering and electron microscopy studies. These experimental small-angle patterns generally display the high-angle sphere form factor peaks but only a single low-angle peak, sometimes accompanied by a much weaker second peak (shoulder). This scattering evidence is still, notwithstanding electron micrographs showing a definite lack of periodic arrangements, taken as indicative of a distorted paracrystalline lattice structure of the spherical domains.[19-23] The purpose of this paper is (i) to show that for some systems the low-angle peaks in small-angle scattering patterns from diblock copolymers can be well explained as arising from the short-range order typical of liquid-like packing of hard-sphere domains and (ii) to obtain the hard-sphere interaction distance of the matrix chains by modeling the small-angle scattering data using a hard-sphere interaction potential and the Percus–Yevick approximation for the direct correlation function. Recently, Cebula et al.[24] and Ottewill[25,26] have applied the Percus–Yevick hard-sphere model to small-angle scattering data of colloidal systems. Since this approach has not yet been applied to block copolymer systems, we present first a review of the small-angle scattering theory pertaining to spheres with liquid-like packing followed by modeling of experimental scattering curves from the literature for a polystyrene–polybutadiene diblock copolymer/polystyrene homopolymer blend and a polystyrene–polybutadiene diblock.

Small-Angle Scattering Theory

For dilute systems, where the scattering particles are separated by large enough distances so that no interference occurs between scattering from different particles, the intensity of scattered radiation is given simply by the product of the number of scatterers, N, and the scattered intensity of a single particle.[27] This can be expressed in a general way as

$$I(Q) = KNP(Q) \tag{1}$$

where Q is the magnitude of the scattering vector, given by

$$Q = \frac{4\pi}{\lambda} \sin \theta \tag{2}$$

$P(Q)$ is the form factor of the particle, and K is a constant that is a function of the type of radiation used and the sample properties. For a homogeneous sphere of radius R the form factor is

$$P(Q) = v_0^2 \Phi^2(QR) \tag{3}$$

where v_0 is the sphere volume and

$$\Phi(QR) = \frac{3}{(QR)^3}[\sin (QR) - QR \cos (QR)] \tag{4}$$

Thus, for a system of N identical spherical particles, the scattered intensity is

$$I(Q) = KNv_0^2 \Phi^2(QR) \tag{5}$$

0024-9297/84/2217-1712$01.50/0

From eq 4, the maxima in the form factor are calculated to occur at

$$QR = 5.76, 9.10, \ldots \quad (6)$$

Therefore, the radius of the sphere can be calculated from the location of the intraparticle peaks in the scattering curve.

As the density of scattering particles increases, interparticle interference becomes significant. In order to include the effect of particle interference on the scattering intensity, Zernike and Prins[28] derived the following equation, valid for monodisperse particles:

$$I(Q) = KNP(Q)S(Q) \quad (7)$$

where $S(Q)$ is the interference factor, given by

$$S(Q) = 1 + 4\pi n \int_0^\infty (g(r) - 1)\frac{\sin (Qr)}{Qr} r^2 \, dr \quad (8)$$

Here, n is the particle number density and $g(r)$ is the radial distribution function describing the arrangement of the particles. Debye[29] solved eq 8 for (dilute) hard gas spheres (i.e., assuming $g(r) = 0$ for $r < 2R$ and $g(r) = 1$ for $r > 2R$)

$$I(Q) = KNv_0^2\Phi^2(QR)[1 - 8nv_0\Phi(2QR)] \quad (9)$$

As Fournet[31] has pointed out, this scattered intensity distribution becomes negative at low angles for hard-sphere volume fractions greater than 0.125. This impossibility is a result of including only two-body interactions and neglecting higher order interactions. In later liquid-state theories $g(r)$ was modified to take into account three-body interactions.[30,32] Fournet obtained the following result for scattered intensity:[31]

$$I(Q) = KNP(Q)[1 - n(2\pi)^{3/2}\epsilon\beta(Q)]^{-1} \quad (10)$$

where ϵ is a factor close to unity and

$$\beta(Q) = \frac{2}{(2\pi)^{1/2}} \int_0^\infty (e^{-\phi(r)/kT} - 1)\frac{\sin (Qr)}{Qr} r^2 \, dr \quad (11)$$

Fournet's formula (eq 10) can also be solved for a system of hard spheres with $\phi(r) = \infty$ for $0 < r < 2R$ and $\phi(r) = 0$ for $r > 2R$:

$$I(Q) = KNv_0^2\Phi^2(QR)[1 + 8nv_0\epsilon\Phi(2QR)]^{-1} \quad (12)$$

At small volume fractions, the Debye and Fournet equations are equivalent but Fournet's formula is more realistic at high packing densities since it includes three-body correlations.

A successful approach for understanding the scattering from simple liquids is to concentrate on the total correlation function, defined as

$$h(r_{12}) = g(r_{12}) - 1 \quad (13)$$

which measures the deviation of the pair distribution function from its background value due to the influence of particle 1 on particle 2 at a distance r_{12}.[33] Ornstein and Zernike[34] first proposed that $h(r_{12})$ could be considered to consist of a direct correlation between particles 1 and 2 and an indirect term by which the correlation is transferred to all of the neighboring particles. This is expressed mathematically as

$$h(r_{12}) = c(r_{12}) + n \int c(r_{13})h(r_{32}) \, d\mathbf{r}_3 \quad (14)$$

The direct correlation function $c(r_{12})$ should be of short-range order since it is a correlation between particles 1 and 2, depending only on the interparticle potential, which will fall off quickly to zero with separation distance.

A useful approximation for the direct correlation function is the Percus–Yevick[35] expression:

$$c(r) \simeq (e^{-\phi(r)/kT} - 1)e^{\phi(r)/kT}g(r) \quad (15)$$

Wertheim[36] and Thiele[37] independently showed that this direct correlation function has an exact closed-form solution for the classical hard-sphere fluid. For $r > R$, where $\phi(r)$ is zero, $c(r)$ will also be zero, while for $r < 2R$, $c(r)$ has the polynomial solution

$$c(r) = -(\alpha + \beta s + \gamma s^3) \quad (16)$$

where

$$\alpha = (1 + 2\eta)^2/(1 - \eta)^4$$
$$\beta = -6\eta(1 + \eta/2)^2/(1 - \eta)^4 \quad (17)$$
$$\gamma = \tfrac{1}{2}\eta(1 + 2\eta)^2/(1 - \eta)^4$$
$$s = r/2R$$

Here, η is the hard-sphere volume fraction $4\pi R^3 n/3$. Combining the Fourier transform of the Ornstein–Zernike equation with the definition of the interference factor (eq 8) yields

$$S(Q) = \frac{1}{1 - nC(Q)} \quad (18)$$

where $C(Q)$ is the Fourier transform of the direct correlation function given by

$$C(Q,R,\eta) = -4\pi \int_0^{2R} (\alpha + \beta s + \gamma s^3)\frac{\sin (Qr)}{Qr} r^2 \, dr \quad (19)$$

This integral is readily evaluated[38,39] to give

$$S(Q,R,\eta) = \frac{1}{1 + 24\eta(G(A)/A)} \quad (20)$$

where $A = 2QR$ and

$$G(A) = \frac{\alpha}{A^2}(\sin A - A \cos A) + \frac{\beta}{A^3}(2A \sin A + (2 - A^2) \cos A - 2) + \frac{\gamma}{A^5}(-A^4 \cos A + 4[(3A^2 - 6) \cos A + (A^3 - 6A) \sin A + 6]) \quad (21)$$

The normalized intensity can then be written as

$$I_N(Q) = \frac{I(Q)}{I(0)} = \frac{S(Q)P(Q)}{S(0)P(0)} \quad (22)$$

but $\Phi(0) = 1$ and $S(0) = 1/\alpha$, so

$$I_N(Q,R,\eta) = S(Q,R,\eta)\Phi^2(QR)\alpha \quad (23)$$

Equation 23 is a further improvement over the Debye expression (eq 9) and that of Fournet (eq 11) since it approximately takes into account correlation between all the (hard sphere) particles in the system and therefore will be particularly useful for high particle densities.

Application of the Percus–Yevick Hard-Sphere Model to Block Copolymers

The block copolymer small-angle scattering curves modeled are samples S/SB_d-3 and SB_d-7 from the SANS investigations of Berney et al.[20] The molecular characteristics of these samples are shown in Table I. Sample S/SB_d-3 is a blend of polystyrene–perdeuterated polybutadiene diblock copolymer (SB_d-3) with homopolystyrene (S1) to give a final polybutadiene weight fraction of 0.143 (volume fraction 0.149). Sample SB_d-7 is a pure diblock sample with a similar polybutadiene weight frac-

Table I
Molecular Characteristics

sample	$\bar{M}_{ns} \times 10^{-3}$	$\bar{M}_{nB} \times 10^{-3}$	wt % B	χ_B	η	R, Å	R_{HS}, Å	$2\Delta R$, Å	R_{gS}, Å
SB_d-3	78	54	0.362						
S/SB_d-3	78/64	54	0.143	0.149	0.30	230	290	120	77
SB_d-7	380	46	0.108	0.114	0.52	205	340	270	170
S1	64								

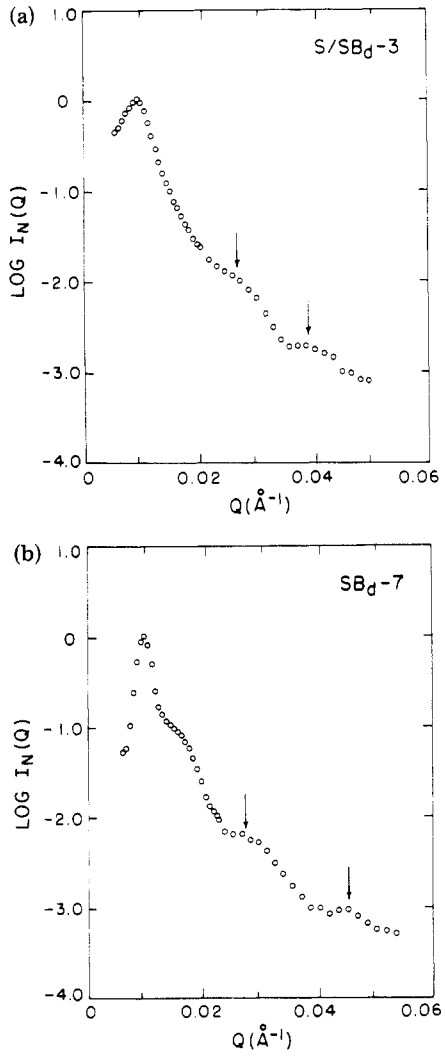

Figure 1. Experimental SANS results taken from Berney et al.:[20] (a) S/SB_d-3; (b) SB_d-7.

tion of 0.108 (volume fraction 0.114). The published electron micrographs of these two samples (see Figure 2 of ref 20) show that the morphology is that of polybutadiene spheres, darkened by osmium tetraoxide staining, in a polystyrene matrix. The spheres do not appear to be ordered.

The small-angle neutron scattering data obtained by Berney et al.[20] for these two samples are reproduced in Figure 1. Sample S/SB_d-3 exhibits a single low-angle interference peak as well as two higher angle sphere form factor peaks (arrows). Sample SB_d-7, on the other hand, has in addition to the low-angle interference peak a weak second interference peak, appearing as a shoulder on the main peak. The peaks at higher angles (arrows) are attributed to intraparticle scattering. The average radii of the polybutadiene spheres were calculated from the assumed intraparticle peaks to be 230 and 205 Å for S/SB_d-3 and SB_d-7, respectively.

Bates et al.[21] attempted to model some of their small-angle neutron scattering results with eq 12 (Fournet) but found a rather poor fit to their data, the calculated curves

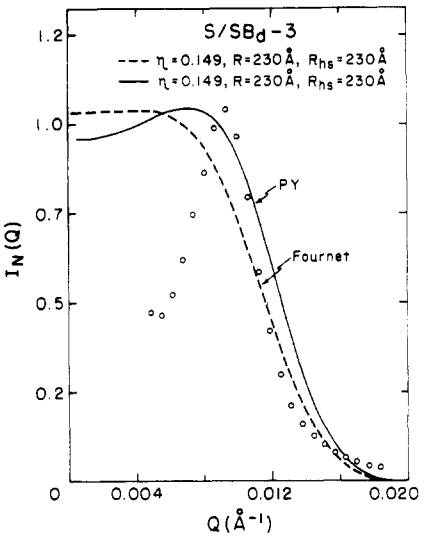

Figure 2. Modeling of scattering from S/SB_d-3 in the low-angle region using Percus–Yevick and Fournet hard-sphere theory with $R_{HS} = R$.

displaying no peak(s) in the low-angle region for the known domain size (calculated from intraparticle peaks and electron microscopy) and volume fraction. As can be seen in Figure 2, application of the Percus–Yevick hard-sphere theory using the same parameters is not substantially better.

Fournet[31] generalized his scattering equation to account for the case where the spherical particles are surrounded by a coat of other molecules (his example: protein molecules surrounded by a layer of water molecules) so that the minimum distance between hard-sphere centers is increased from $2R$ to $2R_{HS}$ and the volume fraction to $(R_{HS}/R)^3\chi$, where χ is the volume fraction of the domain component.

This idea of an impenetrable shell of thickness ΔR surrounding the scattering particles has been found to be quite reasonable for the analysis of the small-angle scattering from microemulsion and colloid systems using Percus–Yevick theory for $S(Q)$.[24-26] The shell corresponds to an adsorbed layer of surfactant or polymer molecules. For spherical domains in diblock copolymers, one would anticipate that the surrounding matrix chains will provide some sort of hindrance to domain–domain approach since they are constrained to have one of their ends (the junction between the two types of blocks) at the surface of the sphere. By assuming a constant domain size (230 Å) but variable hard-sphere size (i.e., with variable η), the data of sample S/SB_d-3 were again fit in the low-angle region for both the Fournet and Percus–Yevick models. As is expected a distinct maximum develops in both the models for high hard-sphere packing fractions. The best fit to the data for the Fournet model occurs for a hard-sphere radius of 350 Å, corresponding to a layer thickness of 120 Å and volume fraction of 0.525, whereas for the Percus–Yevick model, R_{HS} = 290 Å, ΔR = 60 Å, and η = 0.30. Figure 3a shows the full angular range of the scattering predicted by the models using the above parameters along with the experimental data. The experimental and calculated in-

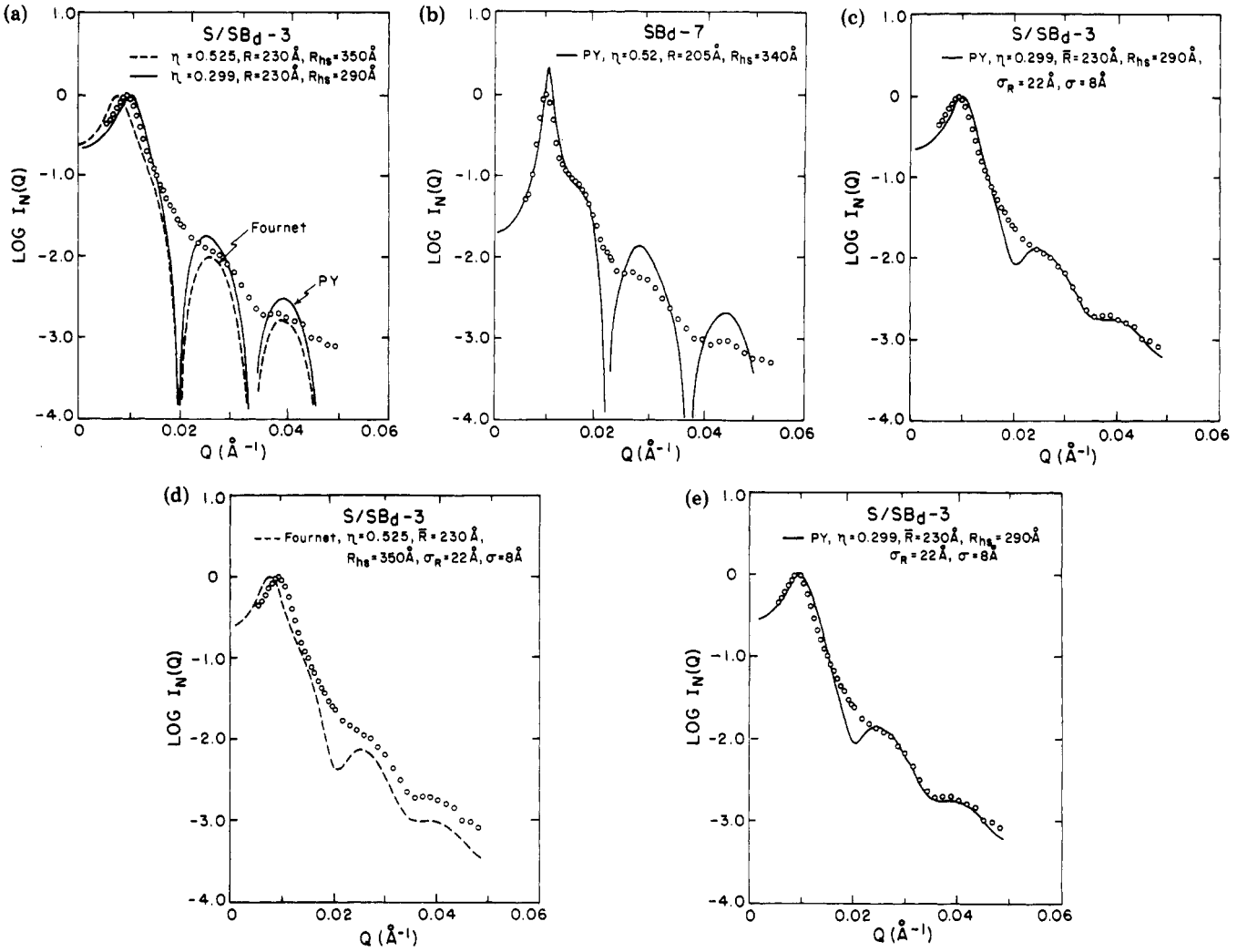

Figure 3. (a) Experimental data vs. Percus–Yevick and Fournet hard-sphere model for S/SB_d-3. (b) Experimental data vs. Percus–Yevick hard-sphere model for SBd-7. (c) S/SB_d-3 experimental data vs. Percus–Yevick hard-sphere model with diffuse boundaries and sphere size distribution in $P(Q)$. (d) S/SB_d-3 experimental data vs. Fournet hard-sphere model with diffuse boundaries and sphere size distribution in $P(Q)$. (e) S/SB_d-3 experimental data vs. Percus–Yevick hard-sphere model with diffuse boundaries and sphere size distribution in both $P(Q)$ and $S(Q)$.

tensities have been respectively normalized by the value of the maximum intensity of the interparticle interference peak. The best fit was determined by visual inspection so that R_{HS} is only accurate to within about 5 Å.

A similar curve-fitting procedure was followed to model the scattering from sample SB_d-7. For this sample, the low-angle peak is considerably sharper, suggesting a very high effective hard-sphere packing fraction. In this case the Percus–Yevick model is appreciably better than the Fournet model, which does not predict a second interference peak even for $\eta = 0.74$. The best fit for the Percus–Yevick model was obtained for $R_{HS} = 340$ Å corresponding to a shell thickness of 130 Å and an effective hard-sphere volume fraction of 0.52.

It should be noted that the diblock copolymer SB_d-1 of ref 21, which exhibits a very highly ordered arrangement of the spherical domains as evidenced by both electron microscopy and SANS (3–4 interparticle interference peaks are seen in addition to sphere form factor peaks), cannot be successfully modeled with the Percus–Yevick hard-sphere model since, even for a hard-sphere volume fraction of 0.74, only two interparticle interference peaks are predicted. Indeed, as Bates has shown[40] the interference peaks can be very well attributed to the lattice peaks of a body-centered cubic lattice (as predicted for spherical domains at equilibrium[11]).

While the relative peak intensities and widths in samples S/SB_d-3 and SB_d-7 are reasonably matched, the zeroes in the theoretical curves are not present in the experimental data, and the experimental sphere form factor scattering peaks are not as intense as predicted. Hashimoto[19] has shown that these details of the higher angle scattering region can be accounted for by introducing a Gaussian distribution in sphere size and a diffuse sphere boundary.

The polydisperse sphere form factor can then be written as

$$P'(Q) = \int_0^\infty P(R) f^2(Q,R)\, dR \Big/ \int_0^\infty P(R)\, dR \qquad (24)$$

Here, $f(Q,R)$ is the scattered amplitude of the spherical particles, modified for the case of diffuse boundaries

$$f(Q,R) = [\tfrac{4}{3}\pi R^3]\Phi(QR) \exp(-\sigma^2 Q^2) \qquad (25)$$

where σ is the parameter that characterizes the diffuseness of the boundary. The electron density profile of the boundary, $\Psi(r)$, is given by a convolution of the density profile for a sharp boundary, $\rho(r)$, with a Gaussian smearing function $k(r)$

$$k(r) = (2\pi\sigma^2)^{-3/2} \exp(-r^2/2\sigma^2) \qquad (26)$$

from which the interfacial thickness t is defined as

$$t = (2\pi)^{1/2}\sigma \quad (27)$$

The function $P(R)$ is normally chosen to be a Gaussian distribution about the average sphere size $\bar{R}$:

$$P(R) = A \exp[-(R - \bar{R})^2/2\sigma_R^2] \quad (28)$$

In their study[20] Berney et al. measured the interface thickness as $t = 22$ Å with $\sigma_R = 22$ Å. Plots c and d of Figure 3 show the improvement in both the Percus–Yevick and Fournet models using these parameters.

The effect of polydispersity on the interference factor should also be considered. Vrij[41] has derived an expression for the scattered intensity from a polydisperse system of homogeneous hard spheres in the Percus–Yevick approximation from which the interference factor can be obtained.[42] For a Gaussian sphere size distribution with a standard deviation less than 10% of the average particle radius, the influence of the polydisperse interference factor on the scattered intensity is very small. The width of the interference peak increases slightly, and its location is shifted to somewhat smaller Q values. Figure 3e shows the predicted scattered intensity, taking the sphere size distribution into account in calculating $S(Q)$.

Discussion

While not illustrated here, both the Percus–Yevick and Fournet scattering models are able to readily fit scattering data with only a single, broad low-angle interference peak. A more stringent test is to fit the intense, relatively narrow peaks in $I(Q)$ which are normally assumed to arise from a paracrystalline arrangement of the domains. The matching of the low-angle interference peak(s) by the Percus–Yevick hard-sphere model using only a single fitting parameter, the hard-sphere radius (or equivalently the hard-sphere volume fraction), is quite impressive. The better accounting of many-body correlations in the Percus–Yevick model makes it superior to the Fournet model for the high (ca. 0.5) range of hard-sphere volume fractions.

Many of the studies on block copolymers with spherical domains find scattering patterns similar in nature to those in Figure 3 but still consider the domains to occupy a distorted paracrystalline simple cubic, body-centered cubic, or face-centered cubic lattice.

At equilibrium the domains in a pure diblock system are predicted to order on a bcc lattice so as to minimize steric repulsions between the matrix chains from different domains.[11,40] Paracrystalline distortions of the domains from their ideal lattice positions, along with a small grain size, are thought to account for the lack of sharpness in the normally observed $S(Q)$. Another argument for (para) crystalline arrangements for spherical domains in diblock/homopolymer blends arises from the belief that a liquid-like array of domains for the low volume fraction of the domain component is incapable of producing a noticeable low-angle scattering maximum (recall model curves in Figure 2).

It is generally accepted that many copolymer systems, particularly those of a spherical morphology, are trapped in a nonequilibrium state characteristic of the temperature/solvent conditions during sample preparation for which molecular mobility abruptly decreased. In addition to poorly ordered domain arrangements, evidence of a trapped nonequilibrium state is the significantly smaller size of the domains in bulk polystyrene–polydiene diblock copolymer systems[19-21] (including those modeled here) than predicted by equilibrium theories.[43] This nonequilibrium effect is observed to be greater for higher molecular weight samples with a glassy matrix component, such as sample SB_d-7, which for all practical purposes never achieve their equilibrium domain size and macrolattice structure. Indeed, the relative spacings of the observed low-angle interference peaks for sample SB_d-7 are 1.00/0.64, which do not correspond to any of the three aforementioned lattices. As Roe[44] has pointed out, there is a general lack of agreement between experimentally determined lattice types for sphere domain macrolattices due in part to the "difficulty of assigning a unique lattice structure when in fact the lattice is not very regular". Moreover, there are electron micrographs that frequently show a disordered array of spheres. Several studies have shown that the addition of homopolymer to the matrix disrupts the ordering of the spherical domains.[20,21] A liquid model is thus physically more realistic for diblock/homopolymer blend systems than for pure diblocks in some nonequilibrium morphology. However, it must be kept in mind that the blend system modeled here has probably not obtained an equilibrium morphology either. Thermodynamic theories[45] for diblock copolymer/homopolymer blends indicate that only a few percent homopolymer with molecular weight comparable to the molecular weight of the matrix block can be solubilized in the matrix phase before the added homopolymer will segregate into its own phase. On the other hand, experimental studies[46] have shown that a much higher amount of homopolymer can be incorporated into the matrix. For example, sample S/SBd-3 contains ~60% homopolystyrene. Meier suggests that the solubilized homopolymer/block copolymer system formed during evaporation of the solvent persists throughout the evaporation and the equilibrium structure is never obtained.[45]

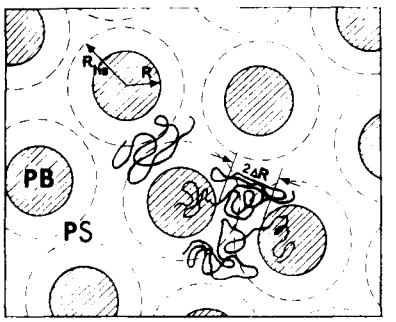

Figure 4. Schematic model of spherical domains with penetrable hard-sphere interactions.

A highly distorted paracrystalline lattice model (Hosemann would suggest an "amorphous lattice" model for a single interference peak[47]) and a liquid-like model are not drastically different in their physical picture of the domain morphology. However, conceptually one approach is to impart disorder to a crystalline lattice until only short-range order remains, while the other approach increases the short-range order intrinsic to liquid-like packing by an increase in the hard-sphere volume fraction. Paracrystalline theory is certainly advantageous in the region of almost-crystalline packing while for simple liquid-like packing, the Percus–Yevick theory is superior; moreover, a rather satisfactory physical interpretation exists for the effective hard-sphere diameter of the spherical domains.

A hard-sphere interaction radius that is larger than the domain radius seems intuitive for a spherical domain structure in a diblock copolymer since each spherical domain has many chains of the matrix component emanating from its surface. However, there is no reason to expect these chains to form an impenetrable shell against other matrix chains from other domains. On the contrary, the matrix chains from each domain will interpenetrate to form a uniform-density matrix (see Figure 4). The limitation on the center-to-center approach distance of the domains

arises from the topological constraints on the matrix chains which have one of their ends (the chemical junction) located on one of the sphere surfaces. The picture that emerges is similar to the problem studied by Meier[48] and Hesselink et al.[49] These authors consider the free energy of interaction between two approaching flat particles bearing polymer adsorbed by one of the chain ends in a solvent medium. They assume that the polymeric layer around the particle to be interpenetrable whereas the particles are impenetrable. In these theories, the total change in free energy per unit area when the two particles approach each other is given by the sum of three terms: a repulsive term due to the loss of configurational entropy, a repulsive term due to the osmotic pressure effect caused by the change in free energy of mixing of polymer and solvent as the density of chain segments changes, and an attractive term due to van der Waals attraction between the flat surfaces. For high surface coverage and high molecular weight of the adsorbed chains, the repulsive forces are dominant, causing a steeply increasing interaction energy with decreasing separation distance near $2R_g$ of the unperturbed chain. Similar repulsive forces should be operative between spheres in a diblock copolymer system during the removal of the solvent. While the interaction potential will not be exactly a hard-sphere potential, if the range of $D_s/2R_{HS}$ over which the interaction potential $\phi(r)/kT$ becomes highly repulsive is small, then a hard-sphere potential becomes a reasonable approximation for modeling purposes. The energy of interaction as a function of interparticle distance has been measured experimentally by Klein et al.[50-52] for flat surfaces bearing adsorbed macromolecules immersed in a solvent (near the Θ condition). A steep repulsion was found for plate separation distances near the unperturbed R_g of the adsorbed molecules. de Gennes[53] has used scaling arguments to discuss the conformation and concentration profiles for long flexible chains grafted at one end to a solid planar surface with the chains immersed in either a good solvent or a solution of the same polymer. For the case of grafted chains in a polymer melt, the conformation of the grafted chain may be extended or stretched normal to the surface for large fractions of grafted surface sites. This same effect should be operative in spherical diblock copolymer/homopolymer systems for the portions of the matrix chains nearest the sphere boundaries causing extended conformations, thus affecting both the distance at which the interdomain interactions become highly repulsive and the steepness of the repulsion.

The dimensions of the penetrable spherical shell, ΔR (see Figure 4), used to model the scattering data can give a direct measurement of the distance between neighboring PB sphere surfaces at which the interdomain potential becomes highly repulsive. For both diblock samples modeled, the distance between neighboring PB sphere surfaces determined from modeling the scattering data ($2\Delta R$) is approximately 1.5 times the unperturbed R_g of the PS matrix chains (see Table I). While no definite conclusions can be drawn from just these two samples, a systematic study of the molecular weight dependence of $2\Delta R$ and the conformation of the matrix chains for diblock copolymer/homopolymer blends exhibiting spherical morphology is being planned for the future.

The use of the Percus–Yevick theory for predicting the direct correlation function is not limited to the case of hard spheres, although this is the only case that can be solved analytically. Of course, it is possible to deduce $\phi(r)$ by Fourier inversion of the scattering data to obtain $g(r)$. Once $g(r)$ is obtained, $c(r)$ and thus $\phi(r)$ follow from eq 13–15. It would be very interesting to compare $\phi(r)$ obtained in this manner to the hard-sphere potential used in the modeling and to that predicted by the thermodynamic theories as well as that deduced from force–separation distance measurements.

Conclusions

Small-angle scattering data from block copolymer systems containing disordered spherical domain structures can be well modeled using the Percus–Yevick hard-sphere liquid theory. By choosing an effective hard-sphere interaction radius based on fitting the lowest angle interference peak position and a domain radius from the higher angle form factor scattering peaks, the full scattering pattern can be quite adequately accounted for, including all peak positions, breadths, and relative intensities. As a consequence of the high hard-sphere density, short-range liquid-like order gives rise to the various low-angle scattering peaks. The difference between the hard-sphere radius and the domain size is attributed to the closest distance of approach between domains and corresponds to about 1.5 times the matrix block chain unperturbed radius of gyration.

Acknowledgment. Financial support from the National Science Foundation, Grant DMR 80-12724 (Polymers Program), and from Union Carbide Corp. is gratefully acknowledged. We also thank Professor E. Kaler of the University of Washington, Dr. D. Handlin, Jr., of Shell Development Co., and Professor T. Hashimoto of Kyoto University for helpful discussions and Dr. F. Bates of AT&T Bell Laboratories for permission to use his experimental scattering data.

Registry No. SB_d-3, 91208-80-9; S1, 9003-53-6.

References and Notes

(1) Szwarc, M.; Levy, M.; Milkovich, R. *J. Am. Chem. Soc.* **1956**, *78*, 2656.
(2) Molau, G. E. "Block Copolymers"; Aggarwal, S. L., Ed.; Plenum Press: New York, 1970; p 79.
(3) Hashimoto, T.; Todo, A.; Itoi, H.; Kawai, H. *Macromolecules* **1977**, *10*, 377.
(4) Gervais, M.; Douy, A.; Gallot, B. *Mol. Cryst. Liq. Cryst.* **1971**, *13*, 289.
(5) Tsouladge, G.; Skoulios, A. *J. Chim. Phys.-Chim. Biol.* **1962**, *59*, 626.
(6) Douy, A.; Gallot, B. *Mol. Cryst. Liq. Cryst.* **1971**, *14*, 191.
(7) Matsuo, M. *Jpn. Plast.* **1968**, *2*, 6.
(8) Kampf, G.; Hoffmann, M.; Kromer, H. *Ber. Bunsenges. Phys. Chem.* **1970**, *74*, 851.
(9) Pedemonte, E.; Turturro, A.; Bianchi, K.; Devetta, P. *Polymer* **1973**, *14*, 145.
(10) Bates, F. S.; Cohen, R. E.; Berney, C. V. *Macromolecules* **1982**, *15*, 589.
(11) Leiber, L. *Macromolecules* **1980**, *13*, 1602.
(12) Inoue, T.; Soen, T.; Kawai, H.; Fukatsu, M.; Kurata, M. *J. Polym. Sci., Part B* **1968**, *6*, 75.
(13) Inoue, T.; Soen, T.; Hashimoto, T.; Kawai, H. *Macromolecules* **1970**, *3*, 87.
(14) Inoue, T.; Soen, T.; Hashimoto, T.; Kawai, H. *J. Polym. Sci., Part A-2* **1969**, *1*, 1283.
(15) Matsuo, M.; Sagae, S.; Asai, H. *Polymer* **1969**, *10*, 79.
(16) Uchida, T.; Soen, T.; Inoue, T.; Kawai, H. *J. Polym. Sci., Part A-2* **1972**, *10*, 101.
(17) Todo, A.; Uno, H.; Miyoshi, K.; Hashimoto, T.; Kawai, H. *Polymer Eng. Sci.* **1977**, *17*, 578.
(18) Kawai, H.; Hashimoto, T.; Miyoshi, K.; Uno, H.; Fujimura, M. *J. Macromol. Sci., Phys.* **1980**, *B17*, 427.
(19) Hashimoto, T.; Fujimura, M.; Kawai, H. *Macromolecules* **1980**, *13*, 1660.
(20) Berney, C. V.; Cohen, R. E.; Bates, F. S. *Polymer* **1982**, *23*, 1222.
(21) Bates, F. S.; Berney, C. V.; Cohen, R. E. *Macromolecules* **1983**, *16*, 1101.
(22) Inoue, T.; Moritani, M.; Hashimoto, T.; Kawai, H. *Macromolecules* **1971**, *4*, 500.

(23) Richards, R. W.; Thomason, J. L. *Polymer* **1981**, *22*, 581.
(24) Cebula, D. J.; Ottewill, R. H.; Ralston, J. *J. Chem. Soc., Faraday Trans. 1* **1981**, *77*, 2585.
(25) Ottewill, R. H. "Colloidal Dispersions"; Goodwin, J. W., Ed.; Royal Society of Chemistry: London, 1982; pp 197-217.
(26) Ottewill, R. H. "Science and Technology of Polymer Colloids"; Poehlein, G. W., Ottewill, R. H., Goodwin, J. W., Eds.; Martinus Nijhoff Publishers: Boston, 1983; NATO ASI Series, Vol. II, pp 503-522.
(27) Guinier, A.; Fournet, G. "Small-Angle Scattering of X-Rays"; Wiley: New York, 1955.
(28) Zernike, F.; Prins, J. A. *Z. Phys.* **1927**, *41*, 184.
(29) Debye, P. *Phys. Z.* **1927**, *28*, 135.
(30) Born, M.; Green, H. S. *Proc. R. Soc. London, Ser. A* **1946**, *188*, 10.
(31) Fournet, P. G. *Acta Crystallogr.* **1951**, *4*, 293.
(32) Rodriguez, A. E. *Proc. R. Soc. London, Ser. A* **1949**, *196*, 73.
(33) Barker, J. A.; Henderson, D. *Rev. Mod. Phys.* **1976**, *43*, 587.
(34) Ornstein, L. S.; Zernike, F. *Proc. Akad. Sci. Amsterdam* **1914**, *17*, 793.
(35) Percus, J. K.; Yevick, G. J. *Phys. Rev.* **1958**, *110*, 1.
(36) Wertheim, M. S. *Phys. Rev. Lett.* **1963**, *10*, 321.
(37) Thiele, E. *J. Chem. Phys.* **1963**, *39*, 474.
(38) Ashcroft, N. W.; Lekner, J. *Phys. Rev.* **1966**, *145*, 83.
(39) Kaler, E. N.; Bennett, K. E.; Davis, H. T.; Scriven, L. E. *J. Chem. Phys.* **1983**, *79* (11), 5673.
(40) Bates, F. S.; Cohen, R. E.; Berney, C. V. *Macromolecules* **1982**, *15*, 589.
(41) Vrij, A. *J. Chem. Phys.* **1979**, *71* (8), 3267.
(42) van Beurten, P.; Vrij, A. *J. Chem. Phys.* **1981**, *74* (5), 2744.
(43) Helfand, E.; Wasserman, Z. *Macromolecules* **1978**, *11*, 960.
(44) Roe, R. J.; Fishkis, M.; Chang, J. C. *Macromolecules* **1981**, *14*, 1091.
(45) Meier, D. J. *Polym. Prepr., Am. Chem. Soc., Div. Polym. Chem.* **1977**, *18*, 340.
(46) Roe, R.-J.; Zin, W. C.; Fishkis, M. IUPAC Proceedings 1982, p 662.
(47) Hosemann, R.; Bagchi, S. W. "Direct Analysis of Diffraction by Matter"; North-Holland Publishing Co. (Amsterdam) and Interscience (New York), 1962.
(48) Meier, D. J. *J. Phys. Chem.* **1967**, *71* (6), 1861.
(49) Hesselink, F. Th.; Vrij, A.; Overbeek, J. Th. G. *J. Phys. Chem.* **1971**, *75* (14), 2094.
(50) Klein, J. *Nature (London)* **1980**, *288*, 248.
(51) Klein, J. *Faraday Trans. 1* **1983**, *79*, 99.
(52) Israelachvili, J. N.; Tirrell, M.; Klein, J.; Almog, Y. *Macromolecules* **1984**, *17*, 204.
(53) de Gennes, P. G. *Macromolecules* **1980**, *13*, 1069.

A Highly Convergent Algorithm for Computing the Orientation Distribution Functions of Rodlike Particles

Judith Herzfeld,*† Alan E. Berger,‡ and John W. Wingate‡

Department of Physiology and Biophysics, Harvard Medical School, Boston, Massachusetts 02115, and Applied Mathematics Branch, Naval Surface Weapons Center, Silver Spring, Maryland 20910. *Received December 13, 1983*

ABSTRACT: A salient difficulty in describing the phase behavior of rodlike particles with large axial ratios or high packing densities has been the solution of the nonlinear integral equation for the orientation distribution function. Approximations that do well for small axial ratios and low packing densities become increasingly unsatisfactory as the axial ratio or the packing density increases. In this report, we demonstrate that solutions of high accuracy may be obtained relatively efficiently by an iterative procedure that converges particularly rapidly for systems with high packing densities and large axial ratios. We show that, for polydisperse as well as monodisperse systems, each iteration moves in a direction of locally decreasing free energy. Although it does not necessarily follow that the net free energy change in a discrete step will be negative, all cases examined thus far generate successive distribution functions with monotonically decreasing free energy.

Introduction

Generalized van der Waals theory has been used with notable success to describe the structure and dynamics of the dense phases of nonassociated systems. (See Chandler et al.[1] for a recent review.) In these materials, intermolecular potentials may be satisfactorily separated into short-ranged repulsions treated as hard-core packing constraints and long-ranged interactions treated in terms of a mean field. One of the limitations in applying this theory to nematic systems has been the difficulty of accurately solving the relevant equations for the particle orientation distribution. In this paper we present an efficient iterative procedure that generates successive particle orientation distributions with monotonically decreasing free energy and converges rapidly to local free energy minima. The procedure also allows for estimation and reduction of the numerical error in the properties calculated from the distribution functions.

According to the van der Waals description, the free energy of N monodisperse rodlike particles with orientations $\Omega = (\theta,\phi)$ ($0 \leq \theta \leq \pi$ and $0 \leq \phi \leq 2\pi$) given by the distribution function $f(\Omega)$ is

$$F\{f(\Omega)\}/NkT = A + \int f(\Omega) \ln f(\Omega)\, d\Omega + \frac{B}{2}\int\int f(\Omega_1)f(\Omega_2) \sin(\gamma_{12})\, d\Omega_1\, d\Omega_2 + \frac{1}{2kT}\int f(\Omega)\psi(\Omega)\, d\Omega \quad (1)$$

where $d\Omega = (1/4\pi) \sin\theta\, d\theta\, d\phi$, γ_{12} is the angle between the axis of a rod with orientation Ω_1 and the axis of a rod with orientation Ω_2, the coefficients A and B are functions of particle asymmetry and particle volume fraction that depend on the model employed for the hard-core reference system, and $\psi(\Omega)$ is the mean field created by long-ranged interparticle forces.[2] In this equation the contributions of orientational entropy (favoring random orientation), translation entropy (favoring alignment), and internal energy (generally also favoring alignment) are represented by the seond, third, and fourth terms, respectively.

Considerations of self-consistency[3] and pair-volume exclusion[4] are satisfied by a mean field of the form

$$\psi(\Omega_1) = \rho\int U(\gamma_{12})f(\Omega_2)\, d\Omega_2 \quad (2)$$

where ρ is the particle number density and $U(\gamma_{12})$ depends

† Harvard Medical School.
‡ Naval Surface Weapons Center.

0024-9297/84/2217-1718$01.50/0